Development of a Calculation Method for Vortex Induced Vibration of a Long Riser Oscillating at its Upper End

Hidetaka SENGA*1,† Wataru KOTERAYAMA*2
senga@riam.kyushu-u.ac.jp

(Received October 31, 2005)

A numerical scheme is developed to simulate three-dimensional dynamics of a flexible riser. Equations of the riser motion are derived based on 'Hamilton's Principle' and solved using the mode expansion method. This scheme was verified by comparing with results of forced oscillation experiments. Finally, to validate the accuracy of this numerical scheme, the numerical and experimental results were compared and showed good agreements.

Key words: *Riser, Vortex induced vibration, Irregular motion, Hamilton's principle, Mode expansion method*

1. Introduction

Risers are used for many purposes such as transporting natural resources from the seabed and lifting cold water for OTEC. They are very long compared with their cross-area section. The stiffness, therefore relatively decreases and risers show very flexible behavior.

One reason that the dynamics of the riser is so complex is the VIV effect induced by the shedding vortices. Even though the maximum amplitude of VIV is small compared with its inline motion, it results in fatigue damage and increases drag forces for inline motion.

Many researchers have investigated experimentally and numerically the VIV of risers. For example, Chung[1] and Whitney[2], and the textbook of Blevins[3] describes a survey of the VIV.

Experimental studies have provided us many useful results. Full-scale experiments were carried out in the Norwegian Deepwater Program, and Halse[4] introduced an overview of the experimental results.

Some researchers solved the VIV using experimental fluid coefficients (Vandiver[5], Otsuka[6], and Etienne[7]) reported a numerical scheme combined with the fluid force and finite element method (FEM). However, a numerical scheme, with which we can calculate the dynamics of such a long flexible riser practically and accurately enough in three-dimension, has not yet been established. From this view point authors have started to study on the dynamics of the riser. In this research, we developed a scheme of three-dimensional dynamics of the riser.

Good agreement between the experimental and numerical result are seen in comparisons.

*1 Department of Earth System Science and Technology, Graduate student
*2 Research Institute for Applied Mechanics, Kyushu University

2. Numerical Scheme

The equations of the riser motion are derived by Hong and Koterayama[8] based on 'Hamilton's Principle' as follows:

In X direction

$$(\tilde{m}+a_X)\{\ddot{u}+z\ddot{\phi}_2+\ddot{X}_0\} +(EIu'')''-(T_e u')'+\mu g\phi_2-Q_X=0 \tag{1}$$

In Y direction

$$(\tilde{m}+a_Y)\{\ddot{v}-z\ddot{\phi}_1+\ddot{Y}_0\} +(EIv'')''-(T_e v')'-\mu g\phi_1-Q_Y=F_L(z,t) \tag{2}$$

In Z direction

$$\tilde{m}\{\ddot{w}+\ddot{Z}_0\}-EA_t w''-\mu g -\{Q_{FX}-Q_{DX}\}\phi_2+\{Q_{FY}-Q_{DY}\}\phi_1-T_0\delta_D(z)=0 \tag{3}$$

In ϕ_1 degree of freedom

$$I\ddot{\phi}_1+\int_0^l\begin{bmatrix}\tilde{m}\{z^2\ddot{\phi}_1-z(\ddot{v}+\ddot{Y}_0)\}+\mu g\{z\phi_1-v\}\\ +z\{Q_{FY}-a_Y(\ddot{v}-z\ddot{\phi}_1+\ddot{Y}_0)-Q_{DY}\}\\ +\delta_D(z)(zR_y-vT_0)\end{bmatrix}dz=0 \tag{4}$$

In ϕ_2 degree of freedom

$$I\ddot{\phi}_2+\int_0^l\begin{bmatrix}\tilde{m}\{z^2\ddot{\phi}_2+z(\ddot{u}+\ddot{X}_0)\}+\mu g\{u+z\phi_2\}\\ +z\{Q_{FX}-a_X(\ddot{u}+z\ddot{\phi}_2+\ddot{X}_0)-Q_{DX}\}\\ -\delta_D(z)(zR_x-uT_0)\end{bmatrix}dz=0 \tag{5}$$

These equations are solved using the mode expansion method. To express the modal functions with $a_i(z)$, satisfying roughly the boundary conditions that top-bottom is simple-free or fixed-free, and the time component of deflections to X and Y direction with $U_i(t)$, $V_i(t)$, deflection variables are replaced as follows:

For simple support

$$a_i(z) = \sin\left(\frac{(2i-1)\pi}{2}\frac{z}{L}\right),\ i = 1,...,N \tag{6}$$

For fixed condition

$$a_i(z) = \sin\left(\frac{(2i-1)\pi}{2}\frac{z}{L}\right),\ i = 1,...,N \tag{7}$$

Deflection variables

$$\begin{cases} u(z,t) + z\phi_2(t) = \sum_{i=1}^{N} a_i(z)U_i(t) \\ v(z,t) - z\phi_1(t) = \sum_{i=1}^{N} a_i(z)V_i(t) \end{cases} \tag{8}$$

As is shown in the textbook written by Blevins, the vortices periodically shed from the cylinder exposed to the free stream flow. The lift forces caused by such shedding vortices affect the cylinder. The strength and period of this lift force are determined by the inline velocity U. Meanwhile, when the top end of a hanging riser moves, each depth of the riser moves with its own amplitude and phase according to the top-end motion. Therefore, the inline velocity at each depth $U(z)$ differ from top to bottom and the lift forces are as follows;

$$F_L(z,t) = \frac{1}{2}\rho U(z)^2 DC_{LY}\sin(\omega_s(z)t) \tag{9}$$

Such various lift forces $F_L(z,t)$ at each depth were introduced into the transverse equation.

3. Model Experiment

A flexible riser model made of polyethylene and Teflon (PTFE) was used in this experiment. Its characteristics are shown in Table 1.

Table 1 Characteristics of the riser model

Model length (m)		6.5
Outer diameter (mm)		22.5
Inner diameter (mm)		12.7
Mass per length (kg/m)		0.4
Young's Modulus (MPa)		8.847
Bottom weight in water (N)		3.489
Natural frequencies of the model (rad/sec)	1st	0.571
	2nd	1.308
	3rd	2.207
	4th	2.732

The natural frequencies of the riser model shown in Table 1 were calculated analytically by solving approximate free vibration equation of the model. The free vibration equation assumes that the bending stiffness effect is small enough to neglect, and this assumption can be adopted for rough calculation of natural frequencies for very flexible riser model (Park[9]).

The dynamics of the model were measured by a three-dimensional motion measurement system using two wing-shaped frames each holding five built-in CCD cameras (Fig. 1)

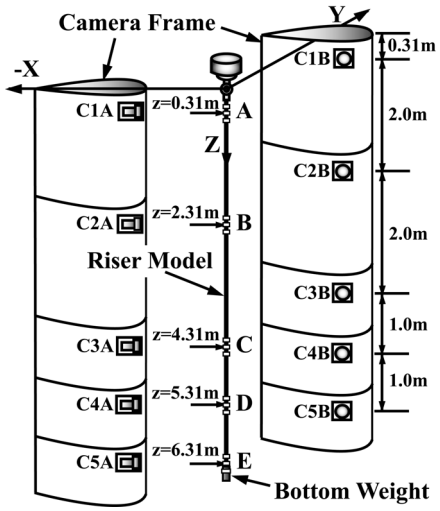

Fig.1 Overview of the measuring system.

The camera C1A ~ C5A and C1B ~ C5B measured the transverse (Y-Z) motion and inline (X-Z plane) respectively.

A parallel mechanism forced oscillator (Yamaguchi[10]) generated irregular motions at the top end of the model. The gap length between the water line and the top end of model was 202 mm, which was 3 percent of the total model length. In the simulation scheme, this gap was treated as not being affected by fluid force. In this experiment, other external forces like wave or current were not generated. Under these conditions, the maximum Reynolds number was 2.0×10^3.

We carried out forced oscillation experiments in still water. The top end of the model was regularly and irregularly oscillated along the X-axis. The inline irregular motion assumes that the floating structure on which the marine riser is installed is affected by ocean waves.

Fig. 2 illustrates this measuring flow of the experiments. For measuring the riser motion CCD cameras are used, of which arrangements are shown in Fig.1, forces and moment are done by using a dynamometer.

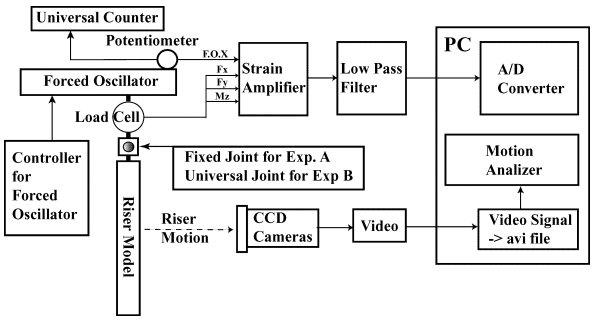

Fig.2 Flowchart for the measurement of the riser motion and force/moment.

4. Experimental and Numerical Results

4.1.1 regular oscillation

At first, results of the numerical simulation and experiments regarding to in-line motion are compared in order to verify the accuracy of the developed simulation scheme.

Figs. 3 shows the inline riser motion response of experimental and simulation results.

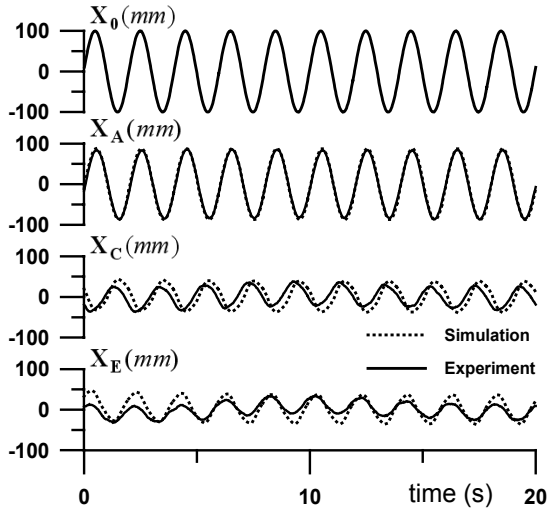

Fig.3a Time series of inline motion (Fixed support).

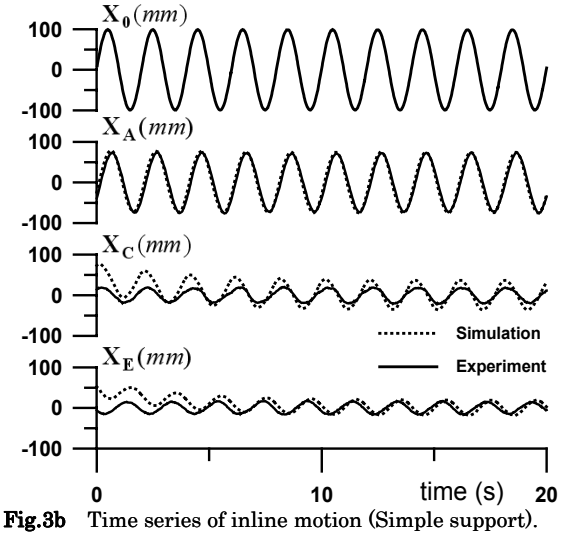

Fig.3b Time series of inline motion (Simple support).

The excitation period is 2.0s, which is the shortest period in experiments, and excitation amplitude is 100mm under Fixed and Simple support boundary condition. This condition of the amplitude and period is very severe for a riser and non-linear effects are expected. The solid lines in the figures are experimental results and dash-dot lines are simulation results. The suffix A~E of X are showing the vertical position of measuring points.

Fig. 4 shows the Configuration profiles of the riser model at A_{X0}=100mm for fixed and simple support

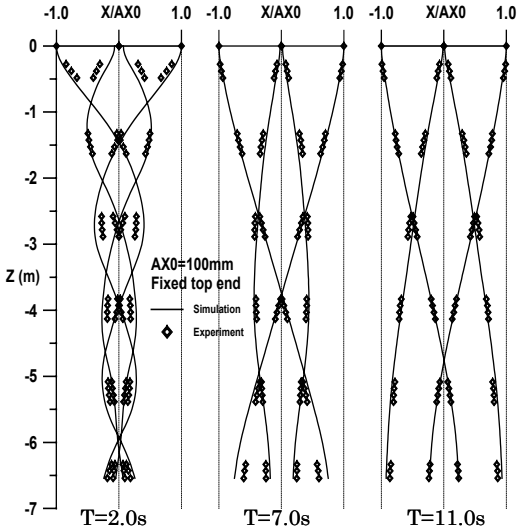

Fig.4a Configuration profiles of the riser (Fixed S.)

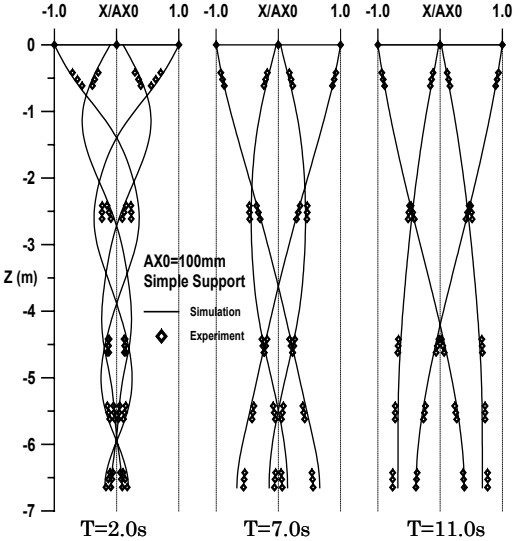

Fig.4b Configuration profiles of the riser (Simple S.)

In Figs. 4, we can see the good agreement between the experimental and numerical results.

Then, to compare the numerical estimations of the share force and moment at the top end of

the model with those of the experimental ones, time histories of top end forces at excitation period of 2.0s and A_{X0}=100mm are shown in Figs. 5.

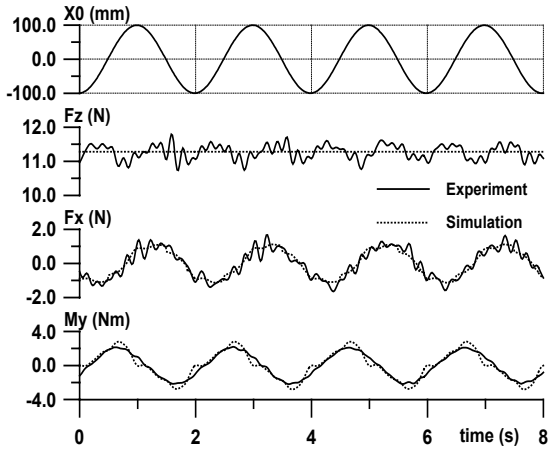

Fig.5a Time histories of top end forces (Fixed support).

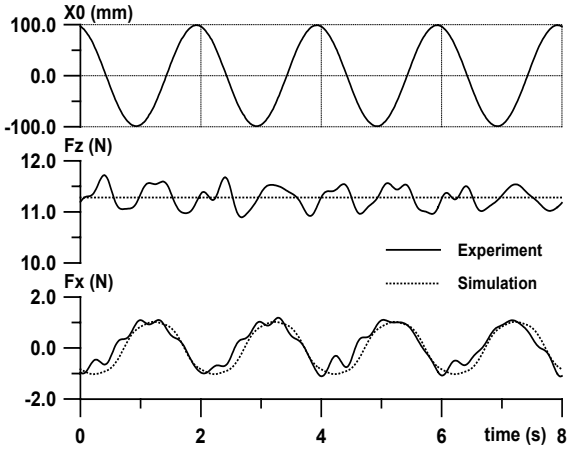

Fig.5a Time histories of top end forces (Fixed support).

In Figs. 5, we can confirm the accuracy of the estimation of share forces and moment.

To show the comparisons of the other experimental conditions, none-dimensional values of the share forces and moment are shown in Figs. 6

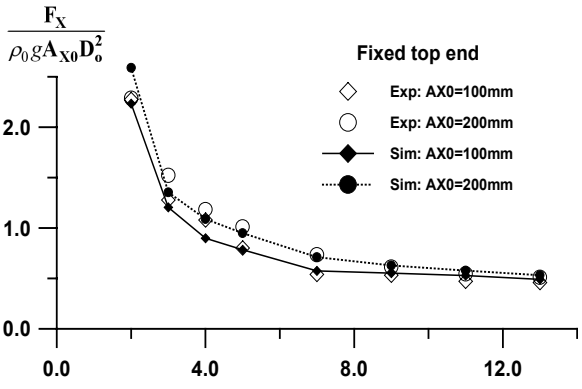

Fig.6a Amplitude of top end force F_X (Fixed support).

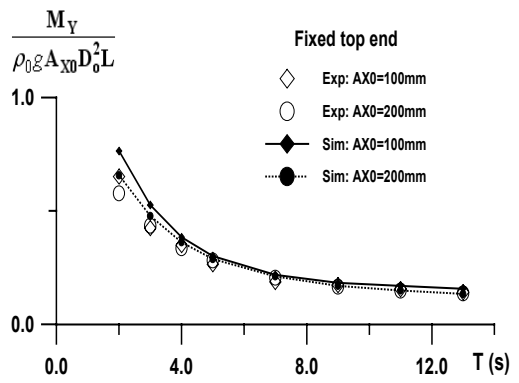

Fig.6b Amplitude of top end moment M_Y (Fixed support).

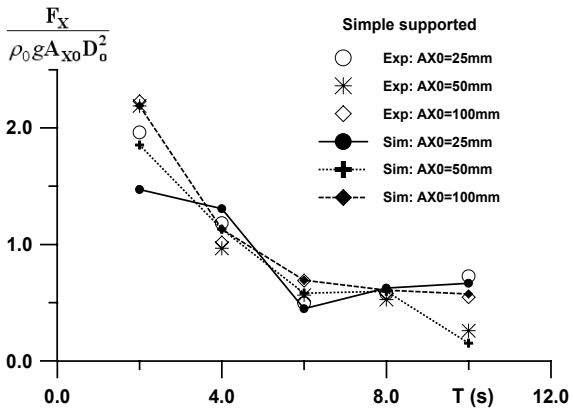

Fig.6c Amplitude of top end force F_X (Simple support).

Figs.3, 4, 5 and 6 verified the accuracy of the numerical simulation scheme for inline motion developed in this study.

4.1.2 Transverse motion

Next, the vortex-induced vibration (transverse motion) is discussed in the case of regular forced oscillation experiments. In these experiment, the boundary condition of the top-bottom of the riser was simple-free.

In order to understand the phenomenon of VIV simply, we classified all experiments into two patterns according to the analysis of the measured transverse motion. One is the case in which a few dominant circular frequencies (ω_s) for the transverse motion exist on one point of the model, and the other is where a single circular frequency dominates the transverse motion from top to bottom. For these two patterns examples, two experiments (T_0= 4sec X_0=100mm, T_0=4sec X_0=50mm) were selected and considered in detail. Figs. 7 show the experimental and simulation results of the time histories of X_0 and the transverse motion at the target points A to E (left side) and their FFT analysis with circular frequency domain (right side) are shown.

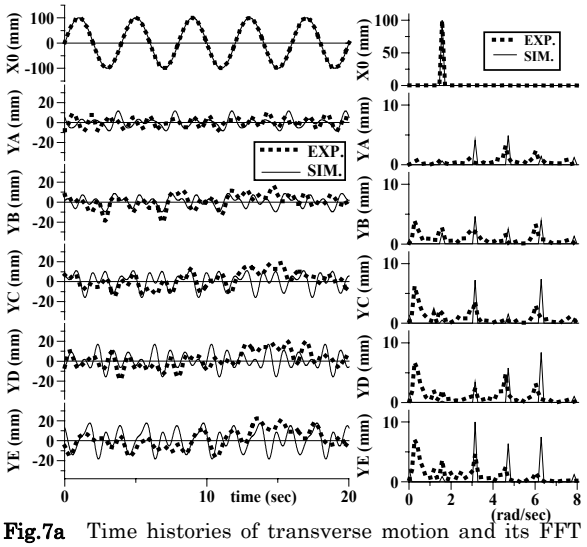

Fig.7a Time histories of transverse motion and its FFT response (X_0=100mm, T_0= 4sec).

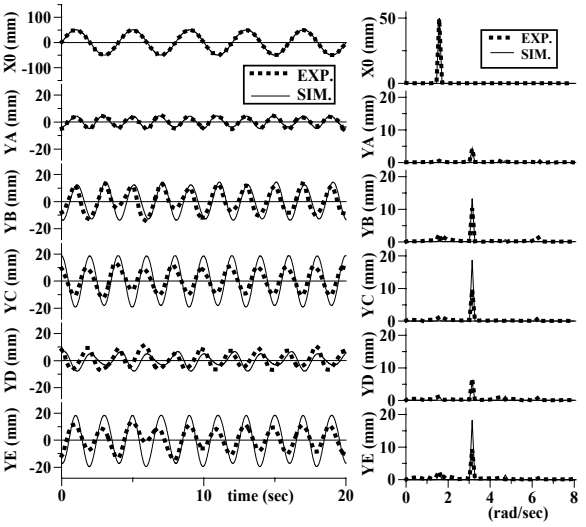

Fig.7a Time histories of transverse motion and its FFT response (X_0=50mm, T_0= 4sec).

From the FFT analysis of Fig. 7a and Fig. 7b, we can confirm that the dominant ω_s is the integral multiples of ω_0; this means that the number of shed vortices during one period of forced oscillation is an even number. For example, $\omega_s/\omega_0=1$ is the case where a pair of vortices is shed, and in $\omega_s/\omega_0=2$, two pair are shed during one period. Because a pair of vortices is likely stable, ω_s is $n\omega_0$ (n=1,2,3,…) so that some even–number vortices are shed during each period of forced oscillation.

Fig. 8 shows configuration profiles of *X-Z* (inline) and *Y-Z* (transverse) plane. At the figure *X-Z* plane, circles show the experimental results at every $T/8$ [sec] and solid lines show the simulation results. At the figure *Y-Z* plane, circles show the measured maximum amplitude at all marked points and solid lines show the simulation results when the amplitude is maximum at points A to E

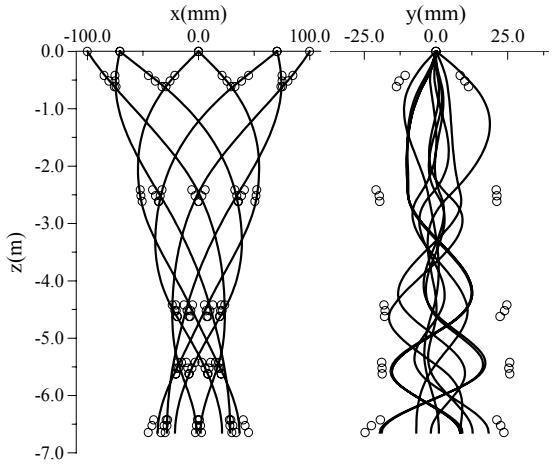

Fig.8a Configuration profiles of the riser (X_0=100mm, T_0= 4sec).

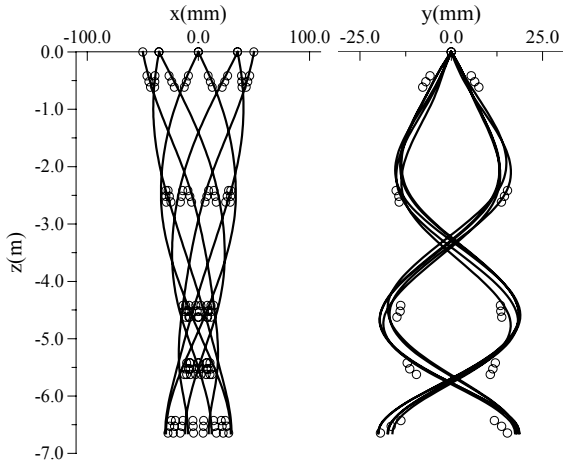

Fig.8b Configuration profiles of the riser (X_0 = 50mm, T_0=4sec).

4.2.1 Irregular oscillation

At first, the time history of inline motion caused by the top-end irregular motion X_0 is shown in Figs. 9.

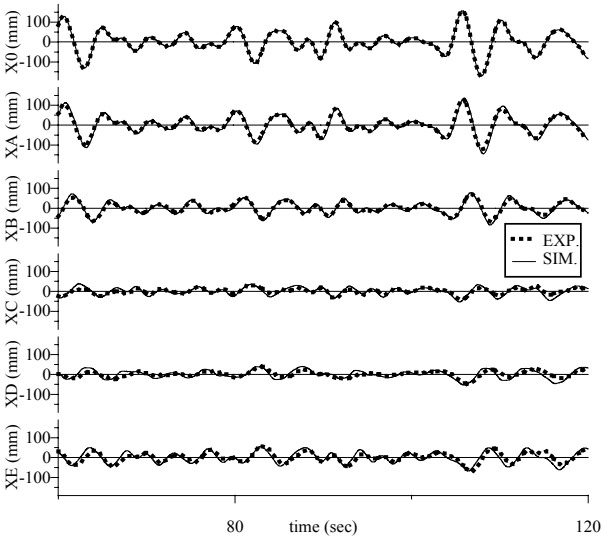

Fig.9a Time histories of inline motion (Mean Period Tx=4.0sec, Significant Amplitude Xw=200mm).

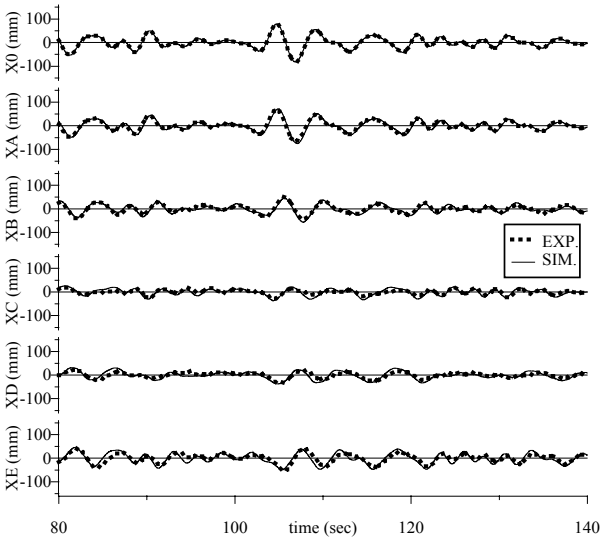

Fig.9b Time histories of inline motion (Mean Period Tx=4.0sec, Significant Amplitude Xw=100mm).

In Figs. 9, the x_A to x_E show the deflection at the selected points A to E, respectively.

The accuracy of this numerical scheme for inline motion of a free hanging riser moving regularly is already mentioned above and Senga and Koterayama[11]. As shown in Figs.9, this numerical scheme also can simulate accurately even if the inline dynamics from top to bottom end of a riser moves irregularly.

Next, the vortex-induced vibration (transverse motion) is discussed in the case of irregular forced oscillation experiments.

The time histories of inline motion X_0 and transverse motion at selected points A to E are shown in Figs.10 and the FFT responses of both results are shown in Figs. 11

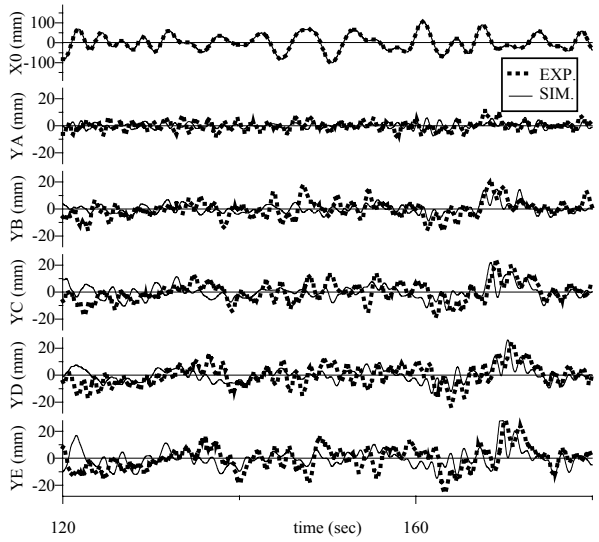

Fig.10a Time histories of transverse motion (Mean Period Tx=4.0sec, Significant Amplitude Xw=200mm).

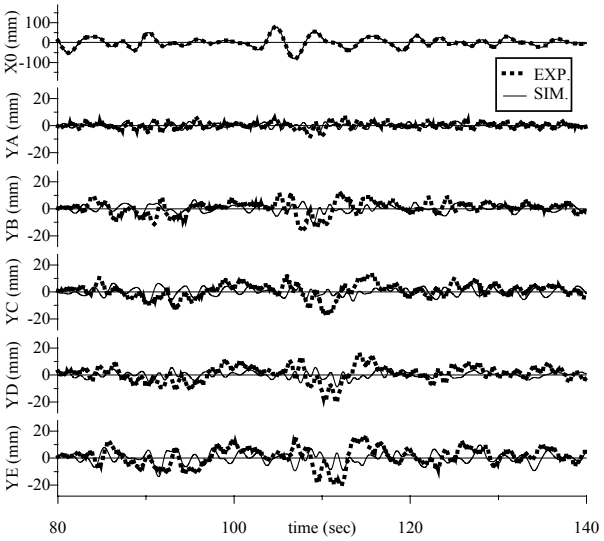

Fig.10b Time histories of transverse motion (Mean Period Tx=4.0sec, Significant Amplitude Xw=100mm).

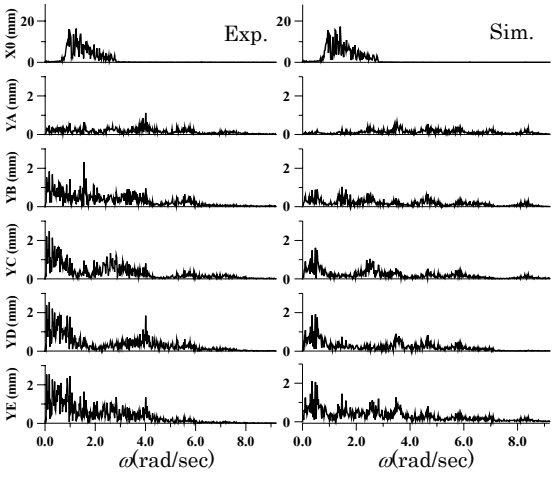

Fig.11a FFT response of transverse motion (Mean Period Tx=4.0sec, Significant Amplitude Xw=200mm).

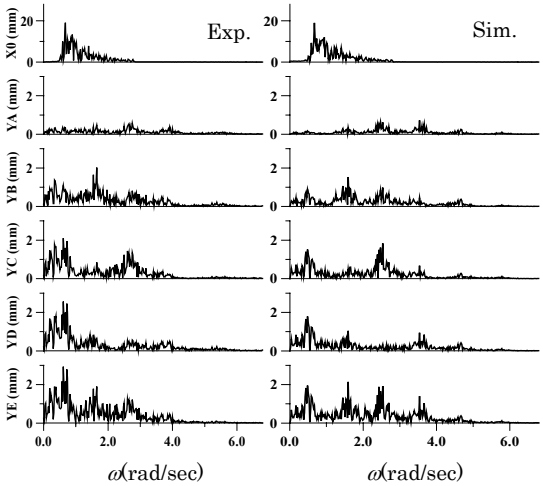

Fig.11b FFT response of transverse motion (Mean Period Tx=4.0sec, Significant Amplitude Xw=100mm).

In Figs. 10, we can see the very similar transverse vibration between the experimental and numerical results. Even though the vibration amplitude is the almost same, there exist parts in which both the results are the opposite motion to the *X*-axis like 140~160 [sec] of right figure. Because the vortex would be shedding in the opposite direction at such a time in the experiment and simulation, the transverse motion became reverse. The direction of transverse motion is accidental and it is not natural to consider as deterministic.

Then, in Fig. 11, we can see some peak frequencies bands exist and they are different at each depth of the model. These regions of peak band are in good agreement with the experimental and numerical results.

To verify the accuracy of the numerical scheme, three examples of significant amplitudes (Yw) and mean periods (Ty) of each point, which calculated from the power spectrum of transverse motions, are compared with experimental results in Table 2.

Table 2 Examples of Significant Amplitude (Yw) and Mean Period (Ty) of transverse motion

Case of large amplitude				
Top end inline motion	Significant Amp. Xw=150mm Mean period Tx=4.0 sec			
Transverse	Yw [mm]		Ty [sec]	
Depth	Exp.	Sim.	Exp.	Sim.
A	11.5	8.4	1.93	1.96
B	19.9	14.6	3.53	2.92
C	23.8	19.3	4.11	3.34
D	24.9	17.6	4.01	4.04
E	29.4	25.7	4.44	3.33
Case of small amplitude				
Top end inline motion	Significant Amp. Xw=100mm Mean period Tx=6.0 sec			
Transverse	Yw [mm]		Ty [sec]	
Depth	Exp.	Sim.	Exp.	Sim.
A	5.00	4.8	3.07	3.11
B	14.5	14.0	4.39	4.46
C	17.0	14.4	5.27	5.22
D	17.1	15.6	8.45	7.65
E	22.6	23.0	5.57	4.91

Calculation results on the case of small forced oscillation amplitude showed better agreements than large forced oscillation case, and this is same tendency as regular forced oscillation experiments as shown in Figs. 8.

4. Summary and Conclusions

To analyze the three-dimensional dynamics of a hanging riser, experiments were carried out using a flexible riser model. The free hanging riser model was forced to oscillate regularly and irregularly at its top end in still water, and its three dimensional motion was measured by CCD cameras. Through the analysis of these experimental results and by comparing the experimental and numerical results, the following conclusions were obtained.

1) The numerical scheme developed in this study brings us very accurate results of surging motion, restoring force and moment regarding to the in-line motion.
2) Regarding to the transverse motion (VIV) the numerical results agree well with experiments except the case of very large forced oscillation amplitude and short period.
3) The peak regions of vibration frequencies of the transverse motion induced by the shedding vortices were in good agreement with experimental results.
4) In the case of very large amplitude and short period forced oscillation experiments, the amplitude of in-line motion decay quickly toward the bottom, and therefore the period of the transverse motion are various along the riser. This makes transverse motion complex and results in inaccuracy of numerical simulation.

References

1) JS. Chung et al., Proc. Offshore Technology Conf, Houston, OTC 3832, pp.341-352, (1980).
2) AK. Whitney et al., J Energy Resources Technology, ASME, Vol. 103, pp.231-236, (1981).
3) RD.Blevins, Flow-induced Vibration, Florida, Krieger Publishing Co., (1990)
4) KH. Halse, Proc 32nd Offshore Tech Conf, Houston, pp.557-564, (2000).
5) JK. Vandiver et al., SHEAR7 program theoretical manual,Dept. of Ocean Engineering, MIT, Cambridge, USA, (1997).
6) K. Otsuka et al., Proc 10th Int Offshore and Polar Eng. Conf, Seattle, Vol. 2, pp.15-22, (2000).
7) S. Etienne et al., Proc. of the 11th Int. Offshore and Polar Eng. Conf., ISOPE, Stavanger, pp.419-425, (2001).
8) YP. Hong and W. Koterayama, Hydroelasticity in Marine Technology 2003, Oxford, UK, pp.37-44, (2003).
9) HI. Park et al., Proc. of the 12th Int. Offshore and Polar Eng. Conf., ISOPE, Kitakyushu, Vol. 2, pp.199-206, (2002).
10) S. Yamaguchi et al., Proc. of the 13th Int. Offshore and Polar Eng. Conf., ISOPE, Honolulu, Vol. 2, pp.186-190, (2003).
11) H. Senga and W. Koterayama, Proc. of the 14th Int. Offshore and Polar Eng. Conf., ISOPE, Toulon, pp.503-510, (2004).